



# Force tracking with feed-forward motion estimation for beating heart surgery

## Citation

Yuen, Shelten G., Douglas P. Perrin, Nikolay V. Vasilyev, Pedro J. del Nido, and Robert D. Howe. 2010. "Force Tracking with Feed-Forward Motion Estimation for Beating Heart Surgery." IEEE Transactions on Robotics 26 (5) (October): 888–896. doi:10.1109/tro.2010.2053734. .

## Published Version

10.1109/TRO.2010.2053734

## Permanent link

<http://nrs.harvard.edu/urn-3:HUL.InstRepos:22085980>

## Terms of Use

This article was downloaded from Harvard University's DASH repository, and is made available under the terms and conditions applicable to Open Access Policy Articles, as set forth at <http://nrs.harvard.edu/urn-3:HUL.InstRepos:dash.current.terms-of-use#OAP>

## Share Your Story

The Harvard community has made this article openly available.  
Please share how this access benefits you. [Submit a story](#).

[Accessibility](#)

# Force Tracking with Feed-Forward Motion Estimation for Beating Heart Surgery

Shelten G. Yuen, Douglas P. Perrin, Nikolay V. Vasilyev,  
Pedro J. del Nido, and Robert D. Howe, *Senior Member, IEEE*

**Abstract**—The manipulation of fast moving, delicate tissues in beating heart procedures presents a considerable challenge to the surgeon. A robotic force tracking system can assist the surgeon by applying precise contact forces to the beating heart during surgical manipulation. Standard force control approaches cannot safely attain the required bandwidth for this application due to vibratory modes within the robot structure. These vibrations are a limitation even for single degree of freedom systems driving long surgical instruments. These bandwidth limitations can be overcome by incorporating feed-forward motion terms in the control law. For intracardiac procedures, the required motion estimates can be derived from 3D ultrasound imaging. Dynamic analysis shows that a force controller with feed-forward motion terms can provide safe and accurate force tracking for contact with structures within the beating heart. *In vivo* validation confirms that this approach confers a 50% reduction in force fluctuations when compared to a standard force controller and a 75% reduction in fluctuations when compared to manual attempts to maintain the same force.

**Index Terms**—force tracking, beating heart surgery, motion compensation, 3D ultrasound, medical robotics

## I. INTRODUCTION

In beating heart procedures, the surgeon operates on the heart while it continues to pump. These procedures eliminate the need for cardiopulmonary bypass and its associated morbidities [1], and allow the surgeon to evaluate the procedure under physiologic loading conditions. The latter is particularly useful in the repair of cardiac structures like the mitral valve that undergo substantial mechanical loads during the heart cycle [2]. However, surgical manipulation of the beating heart is challenging because heart motion exceeds the human tracking bandwidth of approximately one Hz [3]. The mitral valve annulus, for instance, traverses most of its 10–20 mm trajectory and undergoes three direction changes in approximately 100 ms [4]. This makes the application of precise forces for surgical tasks like mitral valve annuloplasty difficult. Indeed, recent animal trials indicate that beating heart repair of the mitral valve cannot be performed reliably due to its fast motion [5].

A force controlled robotic surgical system could benefit the surgeon by applying precise forces to the heart as it moves. Previous work on surgical force control has largely focused on

This work is supported by the US National Institutes of Health under grant NIH R01 HL073647-06. S. G. Yuen and R. D. Howe are with the Harvard School of Engineering and Applied Sciences, Cambridge, MA 02138 USA (e-mail: howe@seas.harvard.edu). Howe is also with the Harvard-MIT Division of Health Sciences & Technology, Cambridge, MA 02139 USA. N. V. Vasilyev, D. P. Perrin and P. J. del Nido are with the Department of Cardiovascular Surgery, Children’s Hospital Boston, MA 02115 USA.

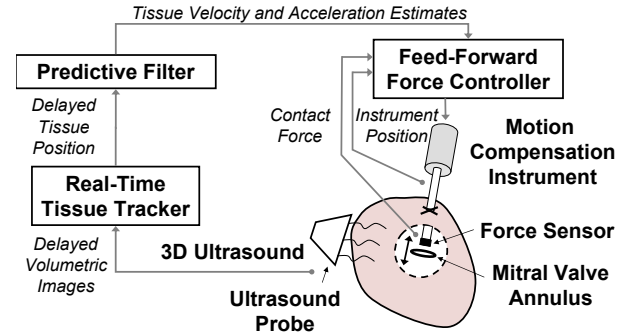


Fig. 1. The surgical system actuates an instrument to apply precise forces against beating heart structures. The controller uses both force measurements and feed-forward tissue motion estimates that are derived from a 3D ultrasound tissue tracker and predictive filter.

force feedback for teleoperation of surgical instruments and robots (reviewed in [6]). Force feedback has demonstrated a number of performance benefits in the execution of remote surgical tasks [7], [8] and can enhance safety when used to implement virtual workspace limits [9]. In this setting, the primary role of the force controller is to provide haptic information to the user while the user commands the robot to interact with the surgical target.

In contrast, beating heart applications require the robot controller to autonomously maintain prescribed forces of the instrument against the target tissue despite its fast motion. One major concern is safety, given the well-documented occurrence of instability in force control [10], [11], [12], [13]. A robotic system for beating heart surgery must be damped and stable to ensure that it will not overshoot or oscillate in response to changes in the desired force trajectory or sudden target motions. Furthermore, the system must have sufficient bandwidth to reject the disturbance caused by heart motion. Previous research indicates that standard force control strategies can only achieve stability for low closed-loop bandwidths due to vibratory modes in the robot structure [11], [12], [13]. These findings were obtained in the context of large industrial robots interacting with stiff targets. To ensure adequate robot performance and safety, it is essential to determine whether the same limitations exist in beating heart surgery where the target is soft but rapidly moving.

In this work, we study force control in the context of beating heart surgery and find that the standard force controller does indeed suffer from bandwidth restrictions due to the vibratory modes present in long surgical instruments. However, by incorporating feed-forward tissue motion information into the

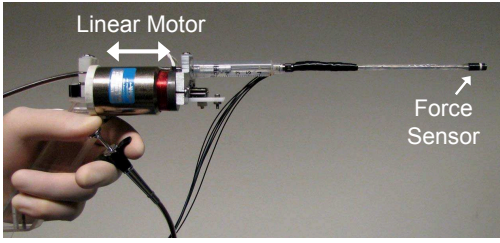


Fig. 2. The motion compensation instrument (MCI) is a handheld surgical anchor deployment device. It is actuated in one degree of freedom to cancel the dominant 1D motion component of the mitral valve annulus. A tip-mounted optical force sensor [15] measures contact forces against beating heart tissue.

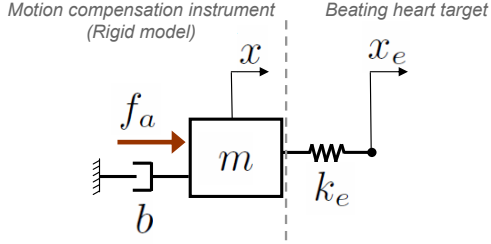


Fig. 3. Rigid body robot model in contact with a moving, compliant environment.

controller, safe and accurate force tracking can be achieved at low bandwidth. In preliminary work we experimentally demonstrated the efficacy of the approach [14], and in the following we provide a detailed analysis of the feed-forward force controller, as well as *in vitro* and *in vivo* validation. In the first part of this paper we show that simultaneously achieving an adequately damped system with good disturbance rejection is challenging because it requires a closed-loop bandwidth that would excite undesired vibratory modes in the robot. Subsequently, we describe a force tracking system that bypasses these bandwidth limitations by using feed-forward heart motion information derived from 3D ultrasound to augment the controller. The system, shown in Fig. 1, is adapted for beating heart mitral valve annuloplasty. It uses a one degree of freedom actuated instrument termed the motion compensation instrument (MCI, Fig. 2) that can follow the rapid, nearly uniaxial motion of the mitral valve annulus [4]. We validate our system and demonstrate its utility to the surgeon in an *in vivo* experiment in a large animal model.

## II. RIGID BODY ANALYSIS

To gain some insight into the use of force control in beating heart surgery, we first consider the case of a perfectly rigid robotic instrument. The robot is modeled as a mass  $m$  and damper  $b$  subjected to a commanded actuator force  $f_a$  and environment contact force  $f_e$ . The damper  $b$  captures the effects of friction in the robot, friction at the insertion point to the heart, and fluid motion. Approximating the environment as a spring of stiffness  $k_e$  yields the system dynamics

$$m\ddot{x} + b\dot{x} = f_a - k_e(x - x_e), \quad (1)$$

where  $x$  is the instrument tip position and  $x_e$  is the desired tissue target position (i.e., its position if it were not deformed

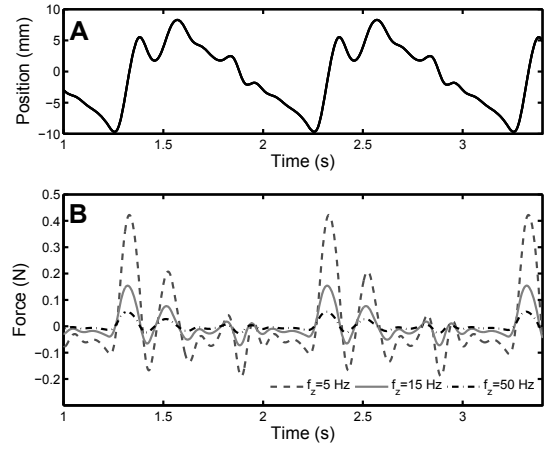


Fig. 4. The effect of mitral valve annulus motion on contact forces. Human mitral valve annulus trajectory (A) and corresponding force disturbances for  $f_z$  of 5, 15, and 50 Hz (B). The mitral annulus has a motion bandwidth of approximately 15 Hz [4]. Gain settings are  $K_f = 27.5$ ,  $K_v = 45.9$  for  $f_z = 5$  Hz;  $K_f = 255.2$ ,  $K_v = 173.8$  for  $f_z = 10$  Hz; and  $K_f = 2845.7$ ,  $K_v = 621.4$  for  $f_z = 50$  Hz. Mitral valve annulus motion data is from [4].

by contact). The model in (1) assumes rigid contact between the instrument and compliant target and is illustrated in Fig. 3. For simplicity, we neglect force sensor compliance in the model because it is significantly stiffer than the tissue environment.

Now consider a standard force regulator control law

$$f_a = f_d + K_f(f_d - f_e) - K_v\dot{x}, \quad (2)$$

where  $K_f$  and  $K_v$  are controller gains and  $f_d$  is the desired force [16]. Combining (1) and (2) and applying the Laplace transform gives the closed-loop contact force relationship

$$F_e(s) = \mathbf{T}(s)F_d(s) + \mathbf{Z}(s)X_e(s), \quad (3)$$

where the force tracking transfer function  $\mathbf{T}(s)$  and robot impedance transfer function  $\mathbf{Z}(s)$  are

$$\mathbf{T}(s) \triangleq \frac{F_e(s)}{F_d(s)} = \frac{\frac{k_e}{m}(1 + K_f)}{C(s)}, \quad (4)$$

$$\mathbf{Z}(s) \triangleq \frac{F_e(s)}{X_e(s)} = -\frac{k_e s(s + \frac{K_v + b}{m})}{C(s)}, \quad (5)$$

$$C(s) = s^2 + \frac{K_v + b}{m}s + \frac{k_e}{m}(1 + K_f). \quad (6)$$

Equation (3) makes explicit that target motion  $x_e$  is a disturbance that perturbs  $f_e$  from  $f_d$ .

Controller gains  $K_f$  and  $K_v$  are chosen to ensure system stability, sufficient damping, and good rejection of  $x_e$ . The last is achieved by designing  $\mathbf{Z}(s)$  to have small magnitude in the bandwidth of  $X_e(s)$ . For the mitral valve annulus, which is bandlimited to approximately 15 Hz [4], this is equivalent to setting the impedance corner frequency  $f_z$  greater than or equal to 15 Hz. Fig. 4 depicts typical mitral valve annulus motion [4] and its effect on the contact force for various  $f_z$  based on simulations of (3)–(5) with  $f_d = 0$ . Parameter values of  $m = 0.27$  kg,  $b = 18.0$  Ns/m, and  $k_e = 133$  N/m are assumed based on system identification of the MCI and preliminary

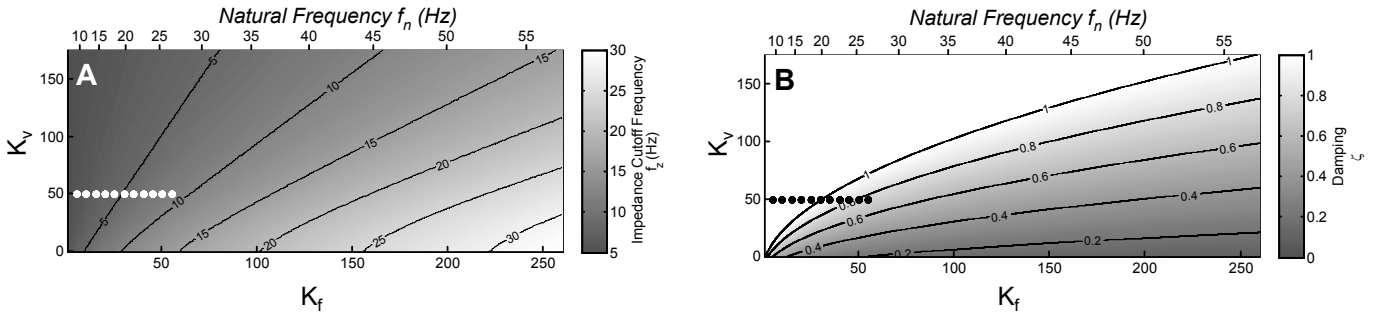


Fig. 5. Impedance corner frequency  $f_z$  (A) and damping  $\zeta$  (B) over different values of  $K_f$  and  $K_v$  using a rigid body model of the MCI. A trade-off exists between damping and disturbance rejection. The natural frequency  $f_n$ , which is related to  $K_f$  through (7), is also shown. Dots indicate the gain test points used for laboratory tests in Section III-B2.

estimates of the mitral valve annulus stiffness. As we will show shortly, obtaining a large impedance corner frequency  $f_z$  is synonymous with increasing the natural frequency  $f_n$  of the closed-loop system, which is also equivalent to increasing  $K_f$ .

The natural frequency  $f_n$  and damping  $\zeta$  of the system can be expressed as

$$f_n = \frac{1}{2\pi} \sqrt{\frac{k_e}{m}(1 + K_f)}, \quad (7)$$

$$\zeta = \frac{K_v + b}{4\pi m f_n}. \quad (8)$$

To avoid potentially dangerous overshoot, we set the system to be critically damped ( $\zeta = 1.0$ ). Manipulating (5), (7), and (8), it can be shown that the natural frequency  $f_n$  of a critically damped system is a function of the impedance corner frequency  $f_z$  by

$$f_n = \left( \frac{\sqrt{208} - 14}{6} \right)^{-\frac{1}{2}} f_z \approx 3.7698 f_z. \quad (9)$$

Hence, while a position regulator can follow a trajectory bandlimited to 15 Hz with about the same closed-loop natural frequency, a force regulator must have a natural frequency of approximately 57 Hz to follow the same motion. This indicates that the force regulator inherently requires high bandwidth to compensate for target motion. From (7)–(9) we calculate gain settings of  $K_f = 255.2$  and  $K_v = 173.8$  to set our system to be critically damped with  $f_z = 15$  Hz, assuming that the rigid body model is appropriate at such high gains. Fig. 5 shows the system damping and impedance corner frequency over a range of values for  $K_f$  and  $K_v$ . It is clear that there is a trade-off between the two performance criteria: increasing  $K_f$  increases the corner frequency but decreases damping; the opposite is true for  $K_v$ . Because of this trade-off, achieving suitable disturbance rejection ( $f_z \geq 15$  Hz) while maintaining damping ( $\zeta \geq 1$ ) requires large gains.

### III. BANDWIDTH CONSTRAINTS DUE TO ROBOT DYNAMICS

In this section, we study the effect of high gains on robot performance. Extensive prior work on force control has delineated a number of instabilities that can arise in attempting to

control forces using multiple degree of freedom robot arms in contact with hard surfaces [11], [12], [13]. In particular, force controllers can excite structural modes in the manipulator, leading to high amplitude force transients at the end effector. These mechanisms do not pertain to this surgical application, where the end effectors tend to be long, rod-like instruments in order to reach patient anatomy through small ports, and tissues are highly compliant.

It is well known, however, that axial motion of such long rods excites transverse vibrations [17]. The dynamics describing this motion are nonlinear and have time varying parameters, but for the purposes of developing effective force controllers it is not necessary to model these dynamics: we need only to determine the frequency at which they become significant so that reasonable bandwidth restrictions can be imposed on the rigid body model and closed-loop system analysis of the preceding section. While structural resonance can be used to enhance performance in some situations, it is typically avoided because inadvertent excitation of the resonance can destabilize the controller, reduce the positional accuracy of the instrument, and cause undue wear to the robot. In the present application, resonance can further cause injury to the patient from the transmission of vibrational energy to the tissue in contact with the robot.

In the following, we analytically and empirically demonstrate that vibration precludes the use of the high gain force regulator suggested in Fig. 5. We first demonstrate that vibration occurs at relatively low frequency for surgical robots with long instruments. Subsequently, we empirically demonstrate that these vibrations are significant in our system and can lead to instability as  $K_f$  is increased until the natural frequency approaches the resonance of the instrument.

#### A. Gain Limit to Avoid Vibration

Consider a cylindrical rod of length  $l$  and radius  $r$  undergoing axial motion while compressed by a force  $f_e$  (Fig. 6). At low velocities and at compressive loads much smaller than the Euler buckling load (i.e.,  $f_e \ll \frac{E\pi^3 r^4}{4l^2}$ ), the fundamental mode of transverse vibration is well approximated by

$$f_1 \approx \frac{3.5156}{4\pi} \sqrt{\frac{E}{\rho}} \left( \frac{r}{l^2} \right), \quad (10)$$

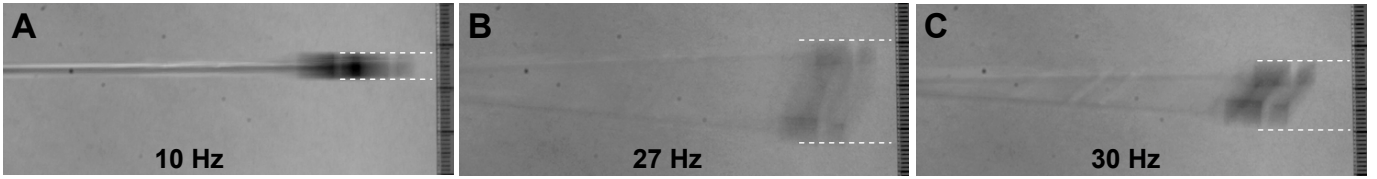


Fig. 7. Instrument with force sensor vibrating due to an axial, sinusoidal motion at 10 Hz (A), 27 Hz (B), and 30 Hz (C) imposed at the base of the instrument shaft. Transverse vibration is maximal at 27 Hz, the predicted resonance frequency from Section III-A. Exposure times are 200 ms. Scale marks at right are in millimeter. Horizontal white dash indicates the displacement extremities.

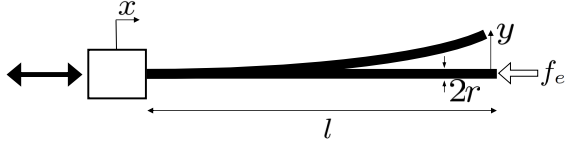


Fig. 6. Axially oscillating cantilevered rod of length  $l$  and radius  $r$ . Lateral motion at the base of the rod ( $x$ ) excites transverse vibrations ( $y$ ) [17].

where  $E$  and  $\rho$  are respectively the Young's modulus and density of the material making up the rod [18]. At large velocities, the fundamental frequency is time varying [17]. At large compressive loads, the fundamental frequency decreases [19]. We omit both of these phenomena for ease of analysis.

The closed-loop natural frequency of the system should be set lower than the first resonance (i.e.,  $f_n < f_1$ ) in order to avoid the effects of vibration. Combining (7) and (10) provides a limit on the proportional gain

$$K_f^{\text{limit}} = \frac{m}{k_e} \left( \frac{3.5156^2 E r^2}{4\rho l^4} \right) - 1. \quad (11)$$

The value of  $K_f$  should be chosen substantially lower than  $K_f^{\text{limit}}$  so that the gain of the closed-loop system is small through the spectral extent of the resonance.

The MCI is mounted with a stainless steel 14 gauge blunt needle ( $E = 200$  GPa,  $\rho = 7900$  kg/m<sup>3</sup>,  $r = 1.1$  mm) with an inner stainless steel push rod used for anchor deployment in mitral valve annuloplasty [20]. Its length is  $l = 22.8$  cm<sup>1</sup>. For simplicity we approximate the entire structure as a solid cylindrical rod. Assuming the same system parameters as before, (10) and (11) predict that the fundamental resonance occurs at  $f_1 = 29.8$  Hz and the limit on the proportional gain is  $K_f^{\text{limit}} = 70.1$ . Referring to the rigid body performance plots in Fig. 5, it is clear that the controller gains cannot be set high enough to simultaneously avoid resonance and meet the criteria of a damped system with high bandwidth.

### B. Experimentally Observed Vibration and Instability

Although avoiding vibratory motion in a surgical robot is intuitively appealing, it remains unclear if such motion is severe enough to present a problem in beating heart surgery. Here we experimentally demonstrate that these vibrations can

affect the accuracy of the instrument tip position and also lead to unstable behavior. We furthermore validate (10) and (11) for predicting the fundamental resonance frequency and gain limit  $K_f^{\text{limit}}$ , respectively.

1) *Characterization of Transverse Vibration Over Frequency*: The MCI was positioned horizontally and clamped along its base to restrict vibrations to only the instrument shaft. The instrument was commanded to follow axial, sinusoidal motion inputs at frequencies between one and 100 Hz. The axial position of the actuator was measured by a high linearity potentiometer (CLP13-50, P3 America, San Diego, CA, USA) at 1 kHz. Transverse vibration of the instrument tip was imaged by a digital camera (EOS 20D, Canon, Tokyo, Japan) with 200 ms exposure time. Vibration amplitudes were measured by a scale placed in the image and oriented to the plane of motion.

Fig. 7 depicts the transverse vibrations observed at 10, 27, and 30 Hz. Large transverse motions are apparent at 27 Hz. Fig. 8 shows the magnitude of the transverse displacement normalized by the magnitude of the axial displacement over frequency. The resonance frequency occurs at 27 Hz, in close agreement with the predicted value from Section III-A. The resonance peaks to a value of 9.8 dB and its effect becomes small at approximately 22.2 Hz. Vibration for inputs with frequencies below 10 Hz and from 50–100 Hz were negligible.

Excitation of the observed resonance would not be safe for beating heart surgery. For context, the mitral valve annulus is a ring of smooth tissue with an approximate width of a few millimeters. Vibration while in contact with the annulus could cause the instrument to slip into the mitral valve or adjacent cardiac structures. Contact with tissue could dampen the vibration but this would also transfer its energy to the patient anatomy and could cause injury.

2) *Force Regulator Instability at High Gain*: In this experiment we study the effect of vibration on stability by testing increasing values of  $K_f$  that approach the predicted  $K_f^{\text{limit}} = 70.1$  from Section III-A. This is equivalent to testing the system at increasing natural frequencies that approach the experimentally observed 27 Hz resonance of the MCI.

As before, the MCI was positioned horizontally on a flat surface and clamped along its body to restrict vibrations to only the instrument shaft. The instrument tip was placed in series with a steel leaf spring with a stiffness matched to the approximate stiffness of the mitral valve annulus ( $k_e = 133$  N/m). The desired force  $f_d$  was a unit step and the MCI was controlled by the force regulator law in (2). Gain values for  $K_f$  ranged from zero to 55 in steps of five and  $K_v$  was

<sup>1</sup>Preliminary animal testing found this to be the minimum length necessary for the instrument to access the mitral valve during beating heart procedures in a porcine model. The instrument approach was from the left atrial appendage through the second intercostal space in a left thoracotomy.

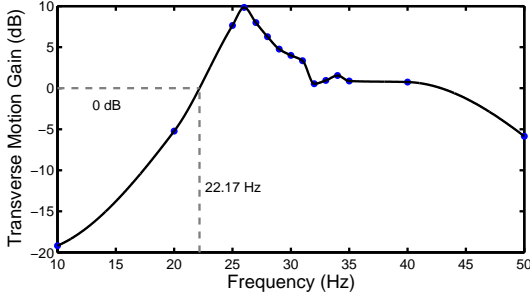


Fig. 8. Magnitude of transverse displacement normalized by the magnitude of the axial displacement ( $y$  and  $x$ , respectively, as shown in Fig. 6). The resonance occurs at 27 Hz, which is near the predicted modal frequency in Section III-A. The estimated 0 dB frequency is marked.

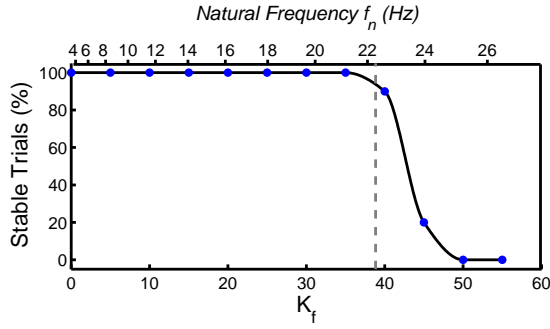


Fig. 9. Stability over increasing proportional gain  $K_f$ . Percentage is taken over 10 trials for each value of  $K_f$ . The natural frequency  $f_n$ , which is related to  $K_f$  through (7), is also shown. The 0 dB corner frequency of the resonance (Fig. 8) is marked with a dashed line and coincides with the onset of instability in the controller.

fixed at 50. These gain values are marked in Fig. 5 to illustrate their locations in the controller design space for a rigid robot. The sample and control frequency was 1 kHz, which is fast enough that approximating the controller as continuous is valid since the effects of discretization are negligible: the plant had a natural frequency of 3.5 Hz and the closed-loop system reached a maximum natural frequency of 26.4 Hz. Ten trials were performed for each gain setting for a total of 120 trials. Controller performance was judged to be stable or unstable for each trial, with the latter criteria defined as exhibiting non-decaying oscillations in excess of 50% overshoot for more than one sec after the unit step input.

Fig. 9 gives the percentage of stable trials over  $K_f$ . As expected, increasing the gain reduces damping and eventually leads to unstable behavior. Instability first arises for 10% of the trials at  $K_f = 40$ , which corresponds to a closed-loop natural frequency of  $f_n = 22.6$  Hz and is nearly coincident with the location of the 0 dB corner frequency for the observed resonance (Fig. 8). Increasing  $K_f$  to 50 and above leads to 100% of the trials being unstable. This is less than the predicted upper bound of  $K_f^{\text{limit}} = 70.1$  but is nonetheless expected because of the spectral width of the resonance seen in Fig. 8. Overall, these results suggest that exciting vibrational modes in even a single degree of freedom robot can lead to an unstable, unsafe controller.

#### IV. FORCE CONTROL WITH FEED-FORWARD TARGET MOTION

The preceding sections indicate that vibrational modes in surgical instruments prevent the high gain settings required for a force regulator to obtain both damping and good heart motion rejection. Rather than use a pure force error feedback control strategy, an alternative strategy employs feed-forward target motion information in the controller. Previous work has shown that this approach can improve force tracking when dealing with moving or uneven surfaces [21]. This approach is well suited to our application because accurate predictions of heart motion can be obtained by exploiting its periodicity [4], [22], [23], [24].

Consider the control law

$$f_a = f_d + K_f(f_d - f_e) + K_v(\hat{x}_e - \dot{x}) + b\hat{x}_e + m\hat{x}_e, \quad (12)$$

which is (2) augmented with feed-forward estimates of the target velocity  $\hat{x}_e$  and acceleration  $\hat{x}_e$ . The contact force relationship in (3) becomes

$$F_e(s) = T(s)F_d(s) - Z(s) \left( X_e(s) - \hat{X}_e(s) \right),$$

where  $T(s)$  and  $Z(s)$  are defined as before in (4) and (5), respectively. Observe that the use of feed-forward terms  $\hat{x}_e$  and  $\hat{x}_e$  enable the cancellation of the motion disturbance  $x_e$  without the need to greatly increase the natural frequency of the system. The controller can then be designed with a low closed-loop natural frequency to avoid the effects of vibration and other high order dynamics that lead to reduced damping and instability. The feed-forward bandwidth is set equal to the bandwidth of the heart motion disturbance, which is lower than the resonance frequency of the robot.

#### V. TISSUE MOTION ESTIMATION WITH 3D ULTRASOUND

Because our surgical application is performed on the mitral valve annulus inside of the beating heart, a real-time imaging technology that can image tissue through blood is required for guidance. We employ 3D ultrasound because it is currently the only technology that meets these criteria while providing volumetric information. To obtain the motion terms needed in the feed-forward controller, we first determine the position of the tissue in the ultrasound volume using the real-time tissue segmentation algorithm from [20]. The algorithm takes advantage of the high spatial coherence of the instrument, which appears as a bright and straight object in the volume, to designate the tissue target. Fig. 10 depicts using this method to track a mitral annulus point in a beating porcine heart.

As in previous work [4], we model the nearly uniaxial motion of the mitral valve annulus as a time-varying Fourier series with an offset and truncated to  $m$  harmonics

$$x_e(t) = c(t) + \sum_{i=1}^m r_i(t) \sin(\theta_i(t)), \quad (13)$$

where  $c(t)$  is the offset,  $r_i(t)$  are the harmonic amplitudes, and  $\theta_i(t) \triangleq i \int_0^t \omega(\tau) d\tau + \phi_i(t)$ , with heart rate  $\omega(t)$  and harmonic phases  $\phi_i(t)$ . Prior to contact, measurements from the tissue tracker are used to train an extended Kalman filter

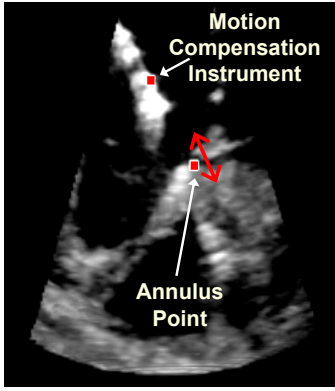


Fig. 10. Slice through real-time 3D ultrasound volume showing tissue tracking. Squares denote the instrument with tip-mounted force sensor and the surgical target located on the mitral valve annulus.

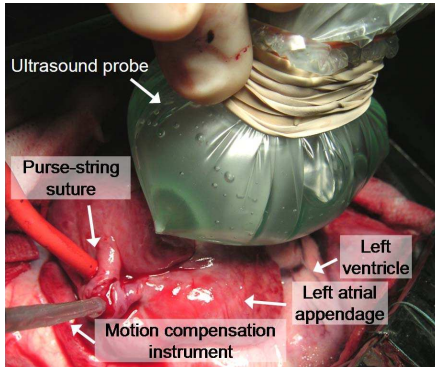


Fig. 11. *In vivo* experiment setup.

to provide estimates of the model parameters  $\hat{c}(t)$ ,  $\hat{r}_i(t)$ ,  $\hat{\omega}(t)$ , and  $\hat{\theta}_i(t)$ . These parameters are used to generate smooth feed-forward velocity and acceleration terms for the force controller of (12) using the derivatives of (13). After contact, filter updates are stopped because the robot interacts with the tissue, causing subsequent position measurements to no longer be representative of the feed-forward (i.e. desired) tissue motion.

## VI. IN VIVO SYSTEM VALIDATION

### A. Experimental Setup

*In vivo* validation of the system was performed in a beating heart Yorkshire pig model (Fig. 11). The tip of the MCI was inserted into the left atrial appendage and secured by a purse-string suture. The 3D ultrasound probe (SONOS 7500, Philips Healthcare, Andover, MA, USA) was positioned epicardially on the free wall of the left ventricle to image the mitral valve and instrument. The probe was placed in a bag with transmission gel to improve contact with the irregular surface of the heart. The surgeon was instructed to hold the instrument tip against the mitral valve annulus with a constant 2.5 N force for approximately 30 sec. This task was performed under three conditions: manually (i.e. fixed instrument with no robot control), using the force regulator in (2), and using the feed-forward force controller in (12). Contact forces were visually displayed to the surgeon during the task and recorded for offline assessment. Three trials were attempted for each

TABLE I  
STANDARD DEVIATIONS OF FORCES IN EACH TRIAL

Trial No.	Manual (N)	Force Regulator (N)	Feed-Forward Force Control (N)
1	0.58	0.23	0.13
2	0.50	0.23	0.09
3	0.37	0.20	0.21

condition. The experimental protocol was approved by the Children's Hospital Boston Institutional Animal Care and Use Committee. The animal received humane care in accordance with the 1996 *Guide for the Care and Use of Laboratory Animals*, recommended by the US National Institute of Health.

In all force controlled trials, the controller gains were designed for  $\zeta = 1.05$ ,  $f_n = 8$  Hz ( $K_f = 4.1$  and  $K_v = 10.5$ ) based on parameter values  $m = 0.27$  kg,  $b = 18.0$  Ns/m, and  $k_e = 133.0$  N/m. The gains were left intentionally low to guarantee controller stability in the unstructured environment of the operating room where off-axis loading could result in instrument bending, as well as to account for uncertainty and variability in heart stiffness. The elastic properties of the heart can vary by a factor of three from patient to patient in normal human hearts and hearts afflicted with congestive cardiomyopathy are on average five times stiffer than the average healthy heart [25].

The force tracking system uses a dual CPU AMD Opteron 285 2.6 GHz PC with 4 GB of RAM to process the ultrasound data and control the MCI. The 3D ultrasound machine streams volumes at 28 Hz to the PC over a 1 Gb LAN using TCP/IP. A program written in C++ retrieves the ultrasound volumes and loads them onto a GPU (7800GT, nVidia Corp, Santa Clara, CA, USA) for real-time beating heart tissue segmentation. This provides tissue position measurements that are used to train the extended Kalman filter. After 5 sec of initialization, the filter outputs estimates of the tissue velocity and acceleration. These are used in tandem with force measurements from a custom, tip-mounted optical force sensor (0.17 N RMS accuracy and 0-4 N range [14], [15]) according to the control law in (12) in a 1 kHz servo loop. As before, the controller was approximated as continuous because the effects of 1 kHz discretization on this 15 Hz bandlimited system is negligible. The MCI is powered by a linear power amplifier (BOP36-1.5 M, Kepco, Flushing, NY, USA).

### B. Results

Fig. 12 provides example force traces for the task executed manually, with the force regulator, and with the feed-forward force controller. Table I lists the force standard deviations for each trial. Averaged across all trials, manual contact with the annulus yielded force standard deviations of  $0.48 \pm 0.06$  N (mean  $\pm$  std error). The force regulator reduced these deviations to  $0.22 \pm 0.01$  N with clear statistical significance in a two-sided t-test ( $p = 0.012$ ). The feed-forward force controller reduced the deviations to approximately 25% of the manual case ( $0.11 \pm 0.02$  N,  $p = 0.017$ ). Statistical significance was also found between the force regulator and feed-forward controller conditions ( $p = 0.009$ ). These results

## VII. DISCUSSION

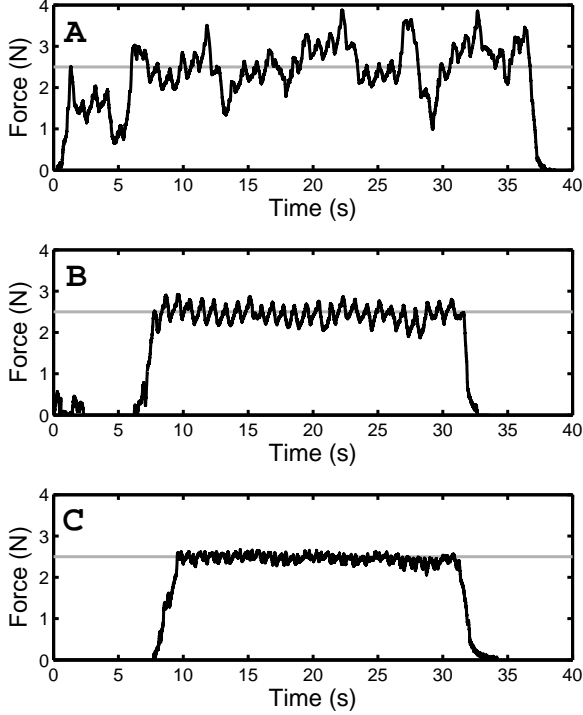


Fig. 12. Example contact force records for manual (A), force regulator (B), and feed-forward force control (C) test conditions. The desired contact force of 2.5 N is indicated (horizontal line). Data was drawn from the trials with the lowest standard deviations.

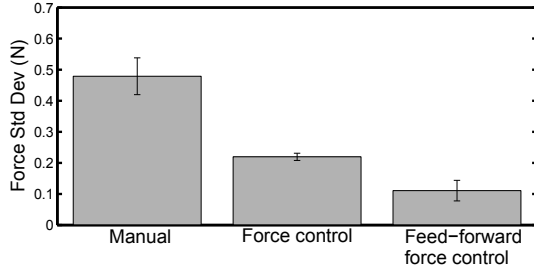


Fig. 13. Disturbance rejection measured by standard deviation of forces. Mean  $\pm$  std error is shown.

are summarized in Fig. 13. The third trial for the feed-forward force controller was omitted from statistical analysis because the animal showed reduced cardiac viability at the end of the experiment. The implications of this result and possible improvements to the surgical procedure are discussed in greater detail in Section VII.

The force regulator and feed-forward force controller also reduced peak-to-peak forces. Manual use of the instrument gave swings in the contact force of  $2.57 \pm 0.29$  N. The force regulator and feed-forward force controller reduced these to  $1.16 \pm 0.10$  N and  $0.65 \pm 0.04$  N, respectively. Statistical significance was found between all conditions at  $p < 0.05$ .

The results from our *in vivo* experiment underscore the benefit of a force controlled robot in beating heart procedures. Without force control, placement of the instrument against the mitral valve annulus gave peak-to-peak force swings of 2.57 N, which is unacceptable compared to the desired 2.5 N force set point. The standard force regulator reduced this fluctuation by 50% and the feed-forward controller reduced it by another 50%. In the case of the feed-forward controller, the precision of the contact forces was 0.11 N. In all of the force controlled experiments, the surgeon expressed greater confidence in instrument manipulation against the beating mitral valve annulus, with the feed-forward controller subjectively better than the standard force regulator. These findings suggest that robotic force control may be an effective aid to the surgeon for beating heart mitral annuloplasty. We note, however, that a potential limitation of the current study is that manual tasks were done with a (nonactuated) motion compensation instrument, which is heavier than typical surgical tools.

The *in vivo* results also verify that safe, precise robotic force tracking is feasible inside of the beating heart through the use of feed-forward target motion information in the controller. This approach enables the robotic system to operate at the motion bandwidth of the heart while simultaneously ensuring damping and providing good disturbance rejection. In contrast, a purely force feedback controller would require a bandwidth approximately 3.8 times higher than the heart motion bandwidth to have the same performance. Our analysis and laboratory experiments indicate that force control at such high bandwidth excites transverse vibrations in the robot that could lead to a variety of dangerous outcomes, including controller instability.

The difficulty in achieving a fast and stable force controller has been examined extensively by other researchers, typically in the industrial setting where large, multiple degree of freedom robots interact with stiff, nearly motionless surfaces. Their analyses found a number of fundamental sources for instability at high bandwidth such as sampling time [10], actuator bandwidth limitations [12], force measurement filtering [12], actuator and transmission dynamics [13], and flexible modes in the robot arm [11], [13]. Recent *in vivo* force control experiments using a multiple degree of freedom endoscopic robot in contact with liver indicate that arm dynamics can limit controller bandwidth to the extent that it is not able to adequately reject slow respiratory motion [26]. For our system and application, the dominant source of instability is from the flexible modes in the surgical instrument. This is somewhat surprising given the simplicity of our robot: basically a small, one degree of freedom actuator mounted with a stiff, nonarticulated rod as an end effector. However, our analysis and experiments confirm that these resonances should and do occur in our robot and are also likely to occur in the instruments mounted to standard surgical robots.

To overcome the bandwidth limitations imposed by vibration, we developed a system that exploits the quasiperiodicity in heart motion to generate feed-forward motion terms for the force controller. Similar approaches have been used for robotic



position tracking of the beating heart. Independently, Ginhoux et al. [23] and Bebek and Cavusolgu [24] have demonstrated that the use of model predictive control can increase the effective tracking bandwidth and positioning accuracy of their multiple degree of freedom robots for coronary artery bypass graft procedures. Our previous work has focused on heart motion prediction to compensate for the time delays and noise inherent in 3D ultrasound-guided, robotic intracardiac procedures [4], [20]. These groups have all demonstrated the *in vivo* feasibility of accurately positioning a robotic instrument relative to a beating heart surgical target. In the current work, we address the successive problem of tracking the heart while applying precise contact forces for surgical manipulation. We pursue this from the perspective of force control and, to the knowledge of the authors, our *in vivo* experiment is the first demonstration of such an approach within the beating heart. Approximately 10 sec of contact are needed to securely place surgical anchors into the annulus. Our *in vivo* experiments demonstrate that the system can control to precise forces for up to at least 20 sec.

A limitation of the current system is that image-based updates of target position are stopped after contact is made because the interaction of the robot with the tissue causes the tissue to deviate from its desired trajectory. In cases of high heart rate variability or arrhythmia, the system would not perform well because tissue motion would not follow the feed-forward model predictions provided by the EKF. This poor performance was observed in the third *in vivo* trial of the feed-forward force controller (Table I). Although not pursued in this work, a clinical workaround may exist for operating on a heart with low motion periodicity: the spontaneous beating of the heart can be slowed through the administration of drugs and then the heart can be electrically paced at a fixed frequency [27]. This may mitigate both heart rate drift and arrhythmia and we believe it would have improved performance for the third *in vivo* trial. This proposed clinical approach is expected to work for most patients experiencing arrhythmia but, as in all surgical procedures, some patients may be ineligible for this beating heart procedure based on the severity of pre-existing conditions.

Finally, we note that there are alternatives to our approach of feeding-forward target motion in order to avoid vibration at high bandwidth. For instance, one could attempt to structurally reinforce the surgical instrument to shift the resonance to higher frequencies, use preshaped command inputs to avoid excitation of the resonance [28], actively control vibration [29], redesign the robot to have a macro-mini actuation scheme so that fast actions are located closer to the instrument tip [30], or use iterative learning control [31]. One could also place a three-axis position sensor on the tip of the instrument, build a nonlinear model to describe the axial-to-transverse coupling dynamics [17], and then attempt the control in a nonlinear controller. Because the stiffness of heart tissue is not known with high accuracy [25], the controller may also have to be designed in the robust or adaptive control frameworks. The plausibility of these approaches should be investigated further. However, a low bandwidth control approach circumvents not just vibration, but all issues that limit or destabilize the

controller at high bandwidth.

#### ACKNOWLEDGEMENT

The authors would like to thank M. Yip for providing the force sensor used in the experiments here and P. Hammer for a number of insightful discussions.

#### REFERENCES

- [1] J. M. Murkin, W. D. Boyd, S. Ganapathy, S. J. Adams, and R. C. Peterson, "Beating heart surgery: why expect less central nervous system morbidity?" *Annals of Thoracic Surgery*, vol. 68, pp. 1498–1501, 1999.
- [2] B. Gersak, "Aortic and mitral valve surgery on the beating heart is lowering cardiopulmonary bypass and aortic cross clamp time," *Heart Surgery Forum*, vol. 5, no. 2, pp. 182–186, 2002.
- [3] V. Falk, "Manual control and tracking – a human factor analysis relevant for beating heart surgery," *Annals of Thoracic Surgery*, vol. 74, pp. 624–628, 2002.
- [4] S. G. Yuen, D. T. Kettler, P. M. Novotny, R. D. Plowes, and R. D. Howe, "Robotic motion compensation for beating heart intracardiac surgery," *International Journal of Robotics Research*, vol. 28, no. 10, pp. 1355–1372, 2009.
- [5] L. K. von Segesser, P. Tozzi, M. Augstburger, and A. Corno, "Working heart off-pump cardiac repair (OPCARE) – the next step in robotic surgery?" *Interactive Cardiovascular and Thoracic Surgery*, vol. 2, pp. 120–124, 2003.
- [6] A. M. Okamura, "Methods for haptic feedback in teleoperated robot-assisted surgery," *Industrial Robot*, vol. 31, no. 6, pp. 499–508, 2004.
- [7] J. Rosen, B. Hannaford, M. P. MacFarlane, and M. N. Sinanan, "Force controlled and teleoperated endoscopic grasper for minimally invasive surgery experimental performance evaluation," *IEEE Transactions on Biomedical Engineering*, vol. 46, no. 10, pp. 1212–1221, Oct 1999.
- [8] C. R. Wagner, N. Stylopoulos, P. G. Jackson, and R. D. Howe, "The benefit of force feedback in surgery: Examination of blunt dissection," *Presence: Teleoperators and Virtual Environments*, vol. 16, no. 3, pp. 252–262, 2007.
- [9] S. C. Ho, R. D. Hibberd, and B. L. Davies, "Robot assisted knee surgery," *IEEE Engineering in Medicine and Biology Magazine*, vol. 4, no. 3, pp. 292–300, 1995.
- [10] D. E. Whitney, "Force feedback control of manipulator fine motions," *Journal of Dynamic Systems, Measurement and Control*, vol. 99, pp. 91–97, 1977.
- [11] S. D. Eppinger and W. P. Seering, "On dynamic models of robot force control," in *Proceedings of the IEEE International Conference on Robotics and Automation*, vol. 3, Apr 1986, pp. 29–34.
- [12] —, "Understanding bandwidth limitations in robot force control," in *Proceedings of the IEEE International Conference on Robotics and Automation*, vol. 4, Mar 1987, pp. 904–909.
- [13] E. Colgate and N. Hogan, "An analysis of contact instability in terms of passive physical equivalents," in *Proceedings of the IEEE International Conference on Robotics and Automation*, vol. 1, May 1989, pp. 404–409.
- [14] S. G. Yuen, M. C. Yip, N. V. Vasilyev, D. P. Perrin, P. J. del Nido, and R. D. Howe, "Robotic force stabilization for beating heart intracardiac surgery," in *Proceedings of Medical Image Computing and Computer-Assisted Intervention (MICCAI 2009)*, vol. 5761, Sept 2009, pp. 26–33.
- [15] M. C. Yip, S. G. Yuen, and R. D. Howe, "A robust uniaxial force sensor for minimally invasive surgery," *IEEE Transactions on Biomedical Engineering*, 2010, accepted.
- [16] B. Siciliano and L. Villani, *Robot Force Control*, 1st ed. Springer, 1999.
- [17] S. H. Hyun and H. H. Yoo, "Dynamic modelling and stability analysis of axially oscillating cantilever beams," *Journal of Sound and Vibration*, vol. 228, no. 3, pp. 543–558, 1999.
- [18] W. Weaver, Jr., S. P. Timoshenko, and D. H. Young, *Vibration Problems in Engineering*, 5th ed. Wiley-Interscience, 1990.
- [19] A. Bokaian, "Natural frequencies of beams under compressive axial loads," *Journal of Sound and Vibration*, vol. 126, no. 1, pp. 49–65, 1988.
- [20] S. G. Yuen, S. B. Kesner, N. V. Vasilyev, P. J. del Nido, and R. D. Howe, "3D ultrasound-guided motion compensation system for beating heart mitral valve repair," in *Proceedings of Medical Image Computing and Computer-Assisted Intervention*, vol. 5241, 2008, pp. 711–719.
- [21] J. De Schutter, "Improved force control laws for advanced tracking applications," in *Proceedings of the IEEE International Conference on Robotics and Automation*, vol. 3, Apr 1988, pp. 1497–1502.

- [22] A. Thakral, J. Wallace, D. Tomlin, N. Seth, and N. V. Thakor, "Surgical motion adaptive robotic technology (s.m.a.r.t.): Taking the motion out of physiological motion," in *Proceedings of Medical Image Computing and Computer-Assisted Intervention*, Oct. 2001, pp. 317–325.
- [23] R. Ginhoux, J. Gangloff, M. de Mathelin, L. Soler, M. M. A. Sanchez, and J. Marescaux, "Active filtering of physiological motion in robotized surgery using predictive control," *IEEE Transactions on Robotics*, vol. 21, no. 1, pp. 27–79, 2005.
- [24] O. Bebek and M. C. Cavusoglu, "Intelligent control algorithms for robotic assisted beating heart surgery," *IEEE Transactions on Robotics*, vol. 23, no. 3, pp. 468–480, Jun. 2007.
- [25] I. Mirsky and W. W. Parmley, "Assessment of passive elastic stiffness for isolated heart muscle and the intact heart," *Circulation Research*, vol. 33, pp. 233–243, 1973.
- [26] N. Zemiti, G. Morel, T. Ortmaier, and N. Bonnet, "Mechatronic design of a new robot for force control in minimally invasive surgery," *IEEE/ASME Transactions on Mechatronics*, vol. 12, no. 2, pp. 143–153, Apr 2007.
- [27] D. Amar, "Prevention and management of perioperative arrhythmias in the thoracic surgical population," *Anesthesiology Clinics*, vol. 26, pp. 325–335, 2008.
- [28] N. C. Singer and W. P. Seering, "Preshaping command inputs to reduce system vibration," *Journal of Dynamic Systems, Measurement, and Control*, vol. 112, no. 1, pp. 76–82, Mar. 1990.
- [29] Z. J. Geng and L. S. Haynes, "Six degree-of-freedom active vibration control using the stewart platforms," *IEEE Transactions on Control Systems Technology*, vol. 2, no. 1, pp. 45–53, 1994.
- [30] M. Zinn, O. Khatib, and B. Roth, "A new actuation concept for human friendly robot design," in *Proceedings of IEEE International Conference on Robotics and Automation*, vol. 1, May 2004, pp. 249–254.
- [31] B. Cagneau, N. Zemiti, D. Bellot, and G. Morel, "Physiological motion compensation in robotized surgery using force feedback control," in *Proceedings of IEEE International Conference on Robotics and Automation (ICRA 2007)*, Apr 2007, pp. 1881–1886.



**Shelten G. Yuen** received a bachelors degree in electrical engineering from the University of California, Davis in 2001, then worked at Agilent Technologies, Inc., Santa Rosa, CA and at MIT Lincoln Laboratory, Lexington, MA from 2001 to 2005. He received a masters degree in applied mathematics and doctorate in engineering sciences from Harvard University in 2007 and 2009. He now is a research scientist at Fitbit, Inc., San Francisco, CA. Dr. Yuen's research interests include applications of estimation, control, and robotics in medicine and

health.



**Nikolay V. Vasilyev** graduated from Moscow Medical Academy. He completed training in cardiovascular surgery at A.N. Bakoulev Center for Cardiovascular Surgery in Moscow. Dr. Vasilyev currently serves as a Staff Scientist at the Department of Cardiac Surgery at Children's Hospital Boston and as an Instructor in Surgery at the Division of Surgery at Harvard Medical School. His research interests include development of beating-heart intracardiac procedures, in particular, new imaging techniques, computer modeling and simulation, and device design.

sign.



**Douglas P. Perrin** received his Ph.D. in 2002 from the University of Minnesota in computer science. His postdoctoral research included surgical robotics, haptics and medical imaging while at the School of Engineering and Applied Science within Harvard University, where he remains an affiliate. Douglas is currently an instructor in surgery at the Harvard Medical School and is a member of the del Nido research group within the the Department of Cardiovascular Surgery at Children's Hospital Boston. His current research interests include image guided beating heart surgery, ultrasound imaging enhancement, and patient specific models for surgical planing.



**Pedro J. del Nido** received his M.D. degree from the University of Wisconsin Medical School. He completed his training at Boston University Medical Center, Toronto General Hospital, and the Hospital for Sick Children in Toronto. Dr. del Nido's basic research is directed at understanding the metabolic and structural changes due to left ventricular hypertrophy. His clinical goal is to apply minimally invasive robotic surgery and other cutting-edge techniques to enhance cardiac surgery.



**Robert D. Howe** is Abbott and James Lawrence Professor of Engineering, Associate Dean for Academic Programs, and Area Dean for Bioengineering in the Harvard School of Engineering and Applied Sciences. Dr. Howe earned a bachelors degree in physics from Reed College, then worked in the electronics industry in Silicon Valley. He received a doctoral degree in mechanical engineering from Stanford University, then joined the faculty at Harvard in 1990. Dr. Howe directs the Harvard BioRobotics Laboratory, which investigates the roles of sensing and mechanical design in motor control, in both humans and robots. His research interests focus on manipulation, the sense of touch, haptic interfaces, and robot-assisted and image-guided surgery.